Cellular Physiology and Biochemistry
Cell Physiol Biochem 2019;52:633-652
DOI: 10.33594/000000045
Published online: 26 March 2019
Accepted: 22 March 2019

Original Paper

Acute Skeletal Muscle Contractions Orchestrate Signaling Mechanisms to Trigger Nuclear NFATc1 Shuttling and Epigenetic Histone Modifications

Frank Suhr[a,b] Kristina Braun[b] Mathias Vanmunster[a] Wilhelm Bloch[b]

[a]Exercise Physiology Research Group, Department of Movement Sciences, Biomedical Sciences Group, KU Leuven, Leuven, Belgium, [b]Institute of Cardiovascular Research and Sport Medicine, Department of Molecular and Cellular Sport Medicine, German Sport University Cologne, Cologne, Germany

Key Words
Ryanodine receptor 1 • Acute exercise • Calcium/calmodulin-dependent protein kinase II • Skeletal muscle • NFATc1 • H3 modifications

Abstract
Background/Aims: Calcium (Ca^{2+}) coordinates skeletal muscle functions by controlling contractions as well as signaling pathways and transcriptional properties. The ryanodine receptor 1 (RyR1), its phosphorylation site (pRyR1Ser^{2840}) and its stabilizers navigate Ca^{2+} oscillations to command muscle signaling cascades and transcriptional activities. While chronic exercise increases pRyR1Ser^{2840}, investigations on acute exercise's effects on RyR1 and Ca^{2+}-dependent modifications of skeletal muscle are rare. The aim of this study was to examine molecular events leading to RyR1 phosphorylation in a physiological model of acute exercise. We hypothesized that exercise-induced RyR1 phosphorylation is associated with altered Ca^{2+}-dependent physiological phenotypes. ***Methods:*** We analyzed pRyR1Ser^{2840}, its stabilizers, involved signaling pathways, and Ca^{2+}-sensitive muscle-determining factors (i.e. NFATc1 and epigenetic histone H3 modifications) in rat muscles upon one single running bout of either concentric or eccentric contractions. ***Results:*** Both acute exercises significantly increased pRyRSer^{2840} levels in muscles, which was accompanied by dissociations of stabilizers from RyR1. Additionally, RyR1 phosphorylation-inducing signaling cascades PTEN/CaMKII/PKA were significantly activated upon exercise. Further, RyR1 phosphorylations were associated with increased Ca^{2+}-dependent NFATc1 nuclear abundances as well as increased Ca^{2+}-dependent epigenetic H3 acetylations pointing to a pRyR1Ser^{2840}-dependent rapid and novel Ca^{2+} equilibrium upon exercise. ***Conclusion:*** Our data report synergistic actions of several distinct pathways to modify RyR1 function to govern physiological phenotypes, here expressed as increased nuclear NFATc1 abundances and epigenetic H3 modifications.

Frank Suhr, PhD
Exercise Physiology Research Group, Department of Movement Sciences, Biomedical Sciences Group
KU Leuven, Tervuursevest 101, 3001 Leuven (Belgium)
Tel. +32 (0) 16 33 06 90, Fax +32 (0) 16 32 91 97, E-Mail frank.suhr@kuleuven.be

Therefore, we underscore the potential of acute exercise to rapidly change muscle Ca^{2+}-controlling systems and downstream effectors cascades to adjust physiological demands for proper muscle function and phenotype adaptation.

Introduction

Coordinated Ca^{2+} oscillations between the sarcoplasmic reticulum (SR) and the sarcoplasm enable physiological skeletal muscle function [1]. As a consequence, chronic alterations in Ca^{2+} oscillations result in reduced muscle contraction and relaxation capabilities [1], are associated with skeletal muscle loss and dysfunction in the elderly [2, 3] and have been reported in patients with skeletal muscle diseases [4–6].

A key mechanism in the skeletal muscle Ca^{2+}-regulating excitation-contraction coupling (ECC) process is the precise regulation of the SR release channel ryanodine receptor isoform 1 (RyR1) [7], which controls SR Ca^{2+} release and thereby maintains physiological cytoplasmic Ca^{2+} concentrations $[Ca^{2+}]_{cyt}$ [3, 8]. RyR1 forms a complex associated with its stabilizers, i.e. calstabin-1 and phosphodiesterase isoform 4D3 (PDE4D3), as well as regulating signaling molecules, i.e. the catalytic subunit of protein kinase A (PKAc), protein phosphastase 1 (PP1) or calcium/calmodulin-dependent protein kinase II (CaMKII) [7, 9]. It has been suggested that chronic (predominantly) concentric exercise induces phosphorylation of human RyR1 at Ser^{2843} (Ser^{2844} in mice/Ser^{2840} in rats) and mediates progressive dissociations of RyR1 stabilizers, eventually resulting in persistently 'leaky' RyR1 [7, 8]. Chronically 'leaky' RyR1s cause uncoordinated Ca^{2+} distributions in myofibers and were proposed to be responsible for reduced skeletal muscle performance in models of muscle diseases [5, 10], in the elderly [3] and after chronic training [8].

We demonstrated that eccentric exercise in humans phosphorylates RyR1 [11]. However, it is unexplored if acute *in vivo* concentric vs. eccentric contractions induce similar or divergent RyR1 modifications and subsequently alterations in sequences of events leading to RyR1 modifications and dissociations of its stabilizing factors. This question is of considerable importance from basic and clinical points of view, as short-termed exercise is a standard to treat muscle-related diseases [12, 13] and to suppress mechanisms of muscle loss in the elderly [2]. Further, repetitive short-termed exercise potentially govern muscle phenotypes by initiating mitochondrial [14] or myosin heavy chain (MyHC)-related [15] gene activities and can increase muscle strength [16]. All these processes rely on altered Ca^{2+} oscillations. Consequently, studies of effects of acute concentric vs. eccentric contractions are needed to understand mechanisms that control Ca^{2+} oscillations and their physiological consequences in skeletal muscles upon acute exercise to optimize (therapeutic) exercise interventions in clinical settings, elderly people, and athletes. Furthermore, pRyR1-induced changes in Ca^{2+} oscillation influence functionally important muscle regulators, i.e. members of the nuclear factor of activated T cell (NFAT). NFATc1 (NFAT2) is controlled by the Ca^{2+}-sensitive phosphatase calcineurin (Cn), which dephosphorylates NFATc1 upon increasing $[Ca^{2+}]_{cyt}$ (resembling altered Ca^{2+} oscillations) to stimulate NFATc1's nuclear translocation by exposing its nuclear localization sequences (NLS). In the nucleus, NFATc1 determines central characteristics of muscle fibers, e.g. myosin heavy chain expression patterns [15, 17]. Another mechanism enabling muscles to adjust their spatiotemporal demands upon exercise are epigenetic histone modifications [18]. Histone H3 acetylations and phosphorylations, both modifications associated by transcriptional initiation and elongation, depend on Ca^{2+}-sensitive kinases, such as CaMKII [19, 20]. Together, NFATc1 and epigenetic H3 modifications illustrate Ca^{2+}-dependent machineries with abilities to rapidly change functional muscle phenotypes.

We hypothesized (i) that acute muscle contractions evoke RyR1 modifications accompanied by RyR1 stabilizer modifications and allied signaling pathways. We hypothesized (ii) RyR1 modifications trigger rapid changes in Ca^{2+}-dependent machineries, i.e. NFATc1 shuttling and H3 modifications, able to rapidly modify functional muscle phenotypes. To this end, we analyzed signaling pathways resulting in RyR1 phosphorylation and molecular changes of RyR1 stabilizers as well as Ca^{2+} oscillations-dependent effectors, i.e. nuclear translocation of NFATc1 and epigenetic H3 modifications in healthy rat muscles upon acute concentric or eccentric running exercise bouts. We report that $pRyR1Ser^{2840}$ levels increased upon acute exercise in a muscle-independent manner. Additionally, we observed exercise-induced increases of RyR1-phosphorylating kinases PKAc and $pCaMKIIThr^{286}$, and importantly, dissociations of RyR1 stabilizers PP1, calstabin-1 and PDE4D3 from RyR1. Functionally, we observed increased nuclear NFATc1 abundances and increased transcription-initiating and –elongating H3 acetylations and phosphorylations upon acute exercise, indicating direct and acute functional consequences of $pRyR1Ser^{2840}$-induced modifications of $[Ca^{2+}]_{cyt}$.

Materials and Methods

Ethical approval

The performed protocols were approved by the ethical committee of the Landesamt für Natur, Umwelt und Verbraucherschutz of North Rhine-Westphalia, Duesseldorf, Germany (reference number: 8.87-50.10.45.08.188).

Animals

Thirty young female Sprague-Dawley rats (13 weeks old, Charles River Laboratories, Boston, U.S.A.) were assigned randomly and in equal numbers (n=10) to the following three intervention groups: control (CON), one single level running exercise bout at +1° treadmill surface angle (1xLevel), and one single downhill running exercise bout at –20° treadmill surface angle (1xDownhill). No statistical differences were observed between the mean body weights of the animals assigned to the different groups (p>0.05, data not shown). Animals were housed in groups of two in standard vivarium cages on a 12:12 light-dark cycle and had *ad libitum* access to standard rat chow and water.

Exercise intervention

The CON group remained sedentary and served as age-matched control. The 1xLevel group performed one single level running exercise bout at 20 $m*min^{-1}$ lasting 15 min at +1° incline, whereas the 1xDownhill group performed one single running exercise bout at 20 $m*min^{-1}$ at -20° decline lasting 15 min. Former studies of our laboratory proved these running conditions as optimal for rat-based interventions [21, 22]. Running sessions were forced by a motor-driven treadmill (Columbus Instruments, Columbus, OH, USA). Vastus lateralis muscles predominantly perform concentric sarcomere shortening during level running and eccentric sarcomere lengthening during downhill running [23]. Hindlimb muscles, including medial gastrocnemius muscles, experience severe muscle damage during downhill running [24, 25], but not during level running, why we propose that medial gastrocnemius muscles (comparable to vastus lateralis muscles) experience eccentric muscle contractions during downhill running. Additionally, we analyzed animals' metabolic turnover by assessing oxygen uptake (VO_2, Columbus Oxymax Economy System, Columbus Instruments, Columbus, OH, USA) under sedentary and both running conditions, because the proportion of eccentric muscle contractions positively correlates with VO_2 due to increased recruitment of motor units [26]. We found significantly increased VO_2 values after both running conditions compared to CON and even higher VO_2 values upon 1xDownhill compared to 1xLevel indicating increased recruitments of motor neurons and thus eccentric contractions during downhill running [26] (Supplementary Fig. S1 - all supplementary material available online at www.cellphysiolbiochem.com). A motor-driven treadmill (Columbus Instruments, Columbus, OH, USA) coupled to the Oymax Economy System was used to increase running velocities during the running test.

Tissue Sampling and Storage

Sedentary animals of the CON group were decapitated after the two-week acclimatization period. Animals of the 1xLevel and 1xDownhill groups were decapitated (30 min post exercise) upon one single running bouts. Both vastus lateralis (LAT) and medial gastrocnemius (GAS) muscles were dissected from the hindlimbs. LAT and GAS muscles from the right hindlimbs were snap-frozen in liquid nitrogen and stored at –80°C until further biochemical analysis. LAT and GAS muscle from the left hindlimbs were immersion-fixed in 4% paraformaldeyde (PFA) and stored –80° until further immunohistochemical analysis.

Transmission electron microscopy

Transmission electron microscopy (TEM) was performed as described earlier [27]. Briefly, skeletal muscle tissue was fixed in 4% PFA, rinsed three times in cacodylate buffer, and then treated with 1% uranyl acetate in 70% ethanol for 8 hrs. After dehydrating the samples in a graded series of ethanol the tissues were embedded in Araldite (Serva). Ultrathin section (60 nm) were processed on an ultramicrotome (Reichert) with a diamond knife and placed on copper grids. TEM was performed with an electron microscope (902A, Carl Zeiss).

Immunohistochemistry and semi-quantitative analysis

The immunohistochemical analyses were performed using standard procedures [11, 28]. Briefly, 4% PFA immersion-fixed 7 µm cryosections were incubated overnight at 4°C with polyclonal primary pRyRSer^{2840} antibody (dilution: 1:100, [11]) Slides were then incubated for 1 hour with appropriate polyclonal biotinylated secondary antibody (diluted 1:400 in 0.05 M Tris-buffered saline, TBS). Afterwards, slides were incubated for 1 hour with streptavidin biotinylated horseradish peroxidase complex (diluted 1:400 in 0.05 M TBS) and stained using a 3, 3`-diaminobenzidine (DAB) solution [11, 28]. LAT and GAS cross sections were stained within a single batch, using the same antibody preparation and the same staining development time to minimize variability in staining efficiency. Digitally captured images (Zeiss Axiophot light microscope coupled to a Sony 3CCD Color Video Camera, 200x magnification) were used to measure RyR1Ser^{2840}-specific staining intensities of each LAT and GAS muscle fibers by selection of the sarcoplasmic region of the myofibers and its subsequent assessment by optical densitometry using a standard software package (ImageJ®, National Institutes of Health, USA) [11]. Intracellular pRyR1Ser^{2840} level was expressed as mean staining intensity. 200 randomly selected fibers of each LAT and GAS and animal were analyzed, resulting in 2000 fibers per intervention group for each LAT and GAS muscles.

Immunofluorescence

Skeletal muscle tissue was prepared as described in the "Immunohistochemistry and semi-quantitative analysis" section. Mouse α-actinin (dilution 1:250) and rabbit pRyR1Ser^{2840} (dilution 1:100) primary antibodies were used. Alexa488 goat anti-mouse (dilution 1:500) and Alexa555 goat anti-rabbit (dilution 1:500) fluorescent secondary antibodies were used. Slides were incubated with the respective primary and secondary antibodies for 1 hour at room temperature. DRAQ5 was used to stain skeletal muscle nuclei [28]. Pictures were taken using a Zeiss confocal laser scanning microscope equipped with a Plan-Neofluar 40x/1.3 Oil DIC objective (LSM 510Meta, Zeiss, Jena, Germany). Alexa488 was exited by an Argon laser using the filter set BP505-530. Alexa555 was exited by a Neon laser using the filter set BP565-615 [28].

Western blot

Upon homogenizing LAT and GAS tissues separately in lysis buffer (Cell Signaling, Frankfurt am Main, Germany), protein concentrations of each homogenate were determined by a protein assay kit (BioRad, Munich, Germany). The general western blot procedure was adapted from laboratory standards [28, 29]. Briefly, 15 µg of total protein were suspended in Laemmli buffer and heated (5 min at 95°C). Linear polyacrylamide gel electrophoresis (PAGE) was performed. Proteins were separated using gels containing either 5% acryl amide (pRyR1Ser^{2840}, and total RyR1), 10% acryl amide (pCaMKIIThr^{286}, pAktSer^{473}, PKAc, PP1, calstabin-1, PDE4D3, GAPDH, and NFATc1) or 15% acryl amide (total H3, H3K9ac, H3K14ac, H3K27ac, and pH3Ser^{10}). Following PAGE, proteins were transferred to polyvinylidene difluoride (PVDF) membranes (Roche, Mannheim, Germany). Membranes were blocked in either 5% low-fat milk (pRyR1Ser^{2840}, RyR1, PKAc, PP1, and calstabin-1) or in 5% bovine serum albumin (pCaMKIIThr^{286}, pAktSer^{473}, PDE4D3, NFATc1, total H3, H3K9ac, H3K14ac, H3K27ac, and pH3Ser^{10}, and GAPDH) for 90 minutes and washed in Tris-buffered saline with 0.1% Tween-20 (pH 7.6). Respective membranes were incubated at 4°C overnight with pRyRSer^{2840}, total RyR1, PKAc, pCaMKIIThr^{286}, pAktSer^{473}, calstabin-1, PP1, PDE4D3, NFATc1, total H3, H3K9ac, H3K14ac, H3K27ac, and pH3Ser^{10}, and GAPDH antibodies (dilutions see Supplementary Table S1). Membranes were incubated with respective secondary horseradish peroxidase antibodies (dilutions see Supplementary Table S1). Proteins were detected by an enhanced chemoluminescence assay (ECL Kit, Amersham-Life Science, Buckinghamshire, UK) and exposed to X-ray film (Kodak X-OMAT Engineering, Eastman Kodak Co., Rochester, NY). Respective bands of each target appeared on X-ray films and were densitometrically measured using Image J (Version 1.43u, National Institutes of Health, Bethesda, USA). GAPDH served as internal loading controls.

Sarcoplasmic reticulum membrane-enriched microsome preparation

To investigate RyR1 assembly, we isolated microsomal proteins from tissue homogenates [9, 30, 31]. To this end, SR membrane-enriched microsomes were prepared as described earlier [9]. Briefly, skeletal muscle homogenates were generated as described in the 'Western blot' section; however, skeletal muscle tissues were homogenized in 3-(N-morpholino)propanesulfonic acid (MOPS) buffer containing 0.9% NaCl, 10 mM MOPS (pH 7.0), and 1 mM PMSF. Upon homogenizing, solutions were centrifuged at 4, 000*g for 15 minutes at 4°C (Eppendorf Centrifuge 5417C, Hamburg, Germany). The supernatant was then collected and further centrifuged at 100, 000*g for 90 minutes at 4°C (Optima TLX Ultracentrifuge equipped with a TLA-55 rotor, Beckman Coulter, Krefeld, Germany). The SR membrane-enriched microsome pellets were resuspended in a buffer containing 0.9% NaCl, 0.3 M sucrose, and 1 mM PMSF [31]. Protein concentrations of pellets and supernatants, respectively, were determined by a protein assay kit (BioRad, Munich, Germany). Relative protein amounts of PKAc, PP1, calstabin-1, and PDE4D3 were measured in pellets and supernatants, respectively, as described in the "Western blot" section.

Nuclear and cytoplasmic fraction isolation from muscle tissue

The protocol was described earlier [32] and slightly modified. Briefly, 100 mg of each LAT and GAS muscle of each condition (CON, 1xLev, 1xDh) were solubilized first in "homogenization" buffer (25 mM HEPES, pH 7.5, 0.5 mM EDTA, 0.5 mM EGTA, 25 mM NaF, 1 mM Na_3VO_4, 1 mM DTT, protease inhibitor [Sigma-Aldrich, Munich, Germany]). After incubating the homogenate for 10 min on ice with regular vortexing, the homogenate was centrifuged for 15 min at 4°C at 22, 000*g. The sarcoplasmic fraction-containing supernatant was stored in a new tubes at -80°C until further analysis, whereas the pellet was washed in "washing" buffer (10 mM HEPES, pH 7.5, 1.5 mM $MgCl_2$, 10 mM KCl, 25 mM NaF, 1 mM Na_3VO_4, 1 mM DTT, protease inhibitor [Sigma-Aldrich, Munich, Germany]). After centrifugation at 3, 000*g for 10 min at 4°C, the supernatant was discarded and the pellet lysed in "solubilization" buffer (20 mM HEPES, pH 7.5, 0.42 M NaCl, 1.5 mM $MgCl_2$, 0.2 mM EDTA, 1% Triton-X 100, 25 mM NaF, 1 mM Na_3VO_4, 1 mM DTT, protease inhibitor [Sigma-Aldrich, Munich, Germany]). The homogenized pellet was stored on ice for 30 min with regular vortexing and centrifuged at 22, 000*g for 20 min at 4°C. The nuclear fraction-containing fraction was stored in a new tube at -80°C until further analysis. Nuclear fractions were identified by total histone H3, whereas sarcoplasmic fractions were identified by GAPDH.

Statistics

Immunohistochemistry and western blot. All data are presented as mean ± S.E.M. Experimental values of the CON groups were used as reference values. One-way analysis of variances (ANOVA) on 'exercise condition' was performed using STATISTICA software package (Statistica for Windows 7.0, Tulsa, USA). If ANOVA was significant, individual differences between tested conditions were analyzed by applying a post hoc test (Duncan's multiple comparison test). Statistical significance was considered for $p<0.05$. To compare PKAc, PP1, calstabin-1, and PDE4D3 values in SR membrane-enriched microsome pellets and supernatants of the respective interventions, paired t-tests were used. Statistical significance was considered for $p<0.05$.

Animal data. To evaluate statistical differences between the investigated groups CON, 1xLevel, and 1xDownhill regarding body weight at the beginning and the end of the study, one-way ANOVA with Duncan's multiple comparison test was conducted. Statistical significance was considered for $p<0.05$.

Results

Eccentric exercise alters sarcomere ultrastructure

First, we analyzed the association between downhill running and predominantly eccentric muscle contractions by transmission electron microscopy (TEM). We did not observe any disruptions of sarcomeric Z-bands after 1xDownhill compared to 1xLevel and CON conditions in either LAT muscles (Fig. 1Aa-c) or GAS muscles (Fig. 1Ad-f), whereas we instead found significantly stretched sarcomeres in LAT (Fig. 1B) and GAS (Fig. 1C) compared to 1xLevel and CON. In addition, we observed irregular M-bands within sarcomeres of 1xDownhill LAT (Fig. 1Ac) and GAS (Fig. 1Af) muscles, which were absent upon CON (Fig. 1Aa, d) and 1xLevel (Fig. 1Ab, e). These data indicate that a single bout of 15 min eccentric running induces higher muscle strain than 15 min of concentric running.

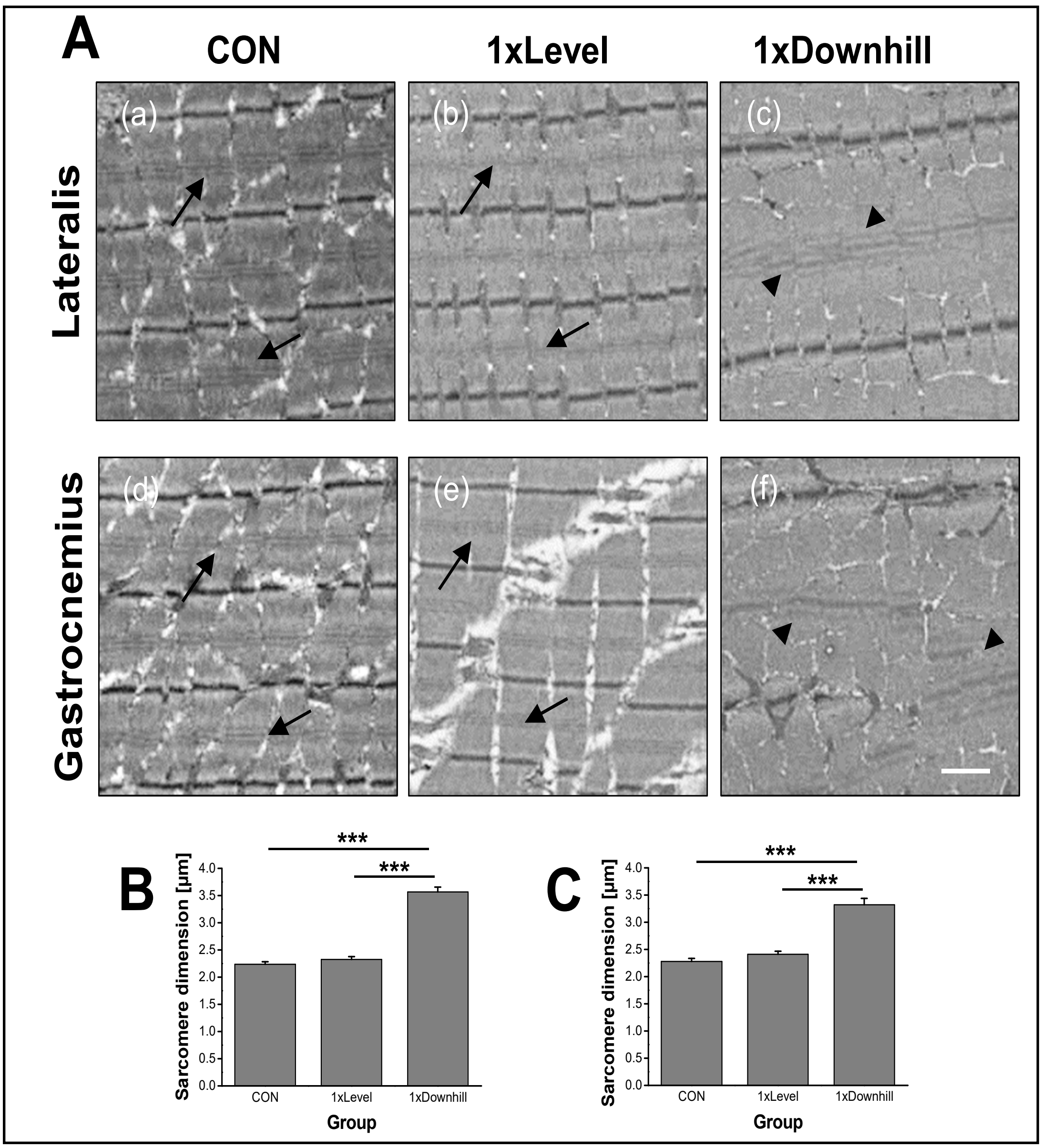

Fig. 1. Transmission electron microscopy (TEM) analysis of concentrically and eccentrically stressed muscle. (A) TEM reveals increased skeletal muscle M-band dilations (see arrow heads) after 1xDownhill compared to 1xLevel and CON conditions, which showed normal M-bands (arrows). (B, C) Quantitative analysis of sarcomeric M-band dimensions in LAT and GAS muscles and the three intervention groups demonstrates significantly increased M-band dimensions upon acute eccentric running. *** p<0.001, bar is 1 µm. Muscles from n=8 rats of each group were analyzed.

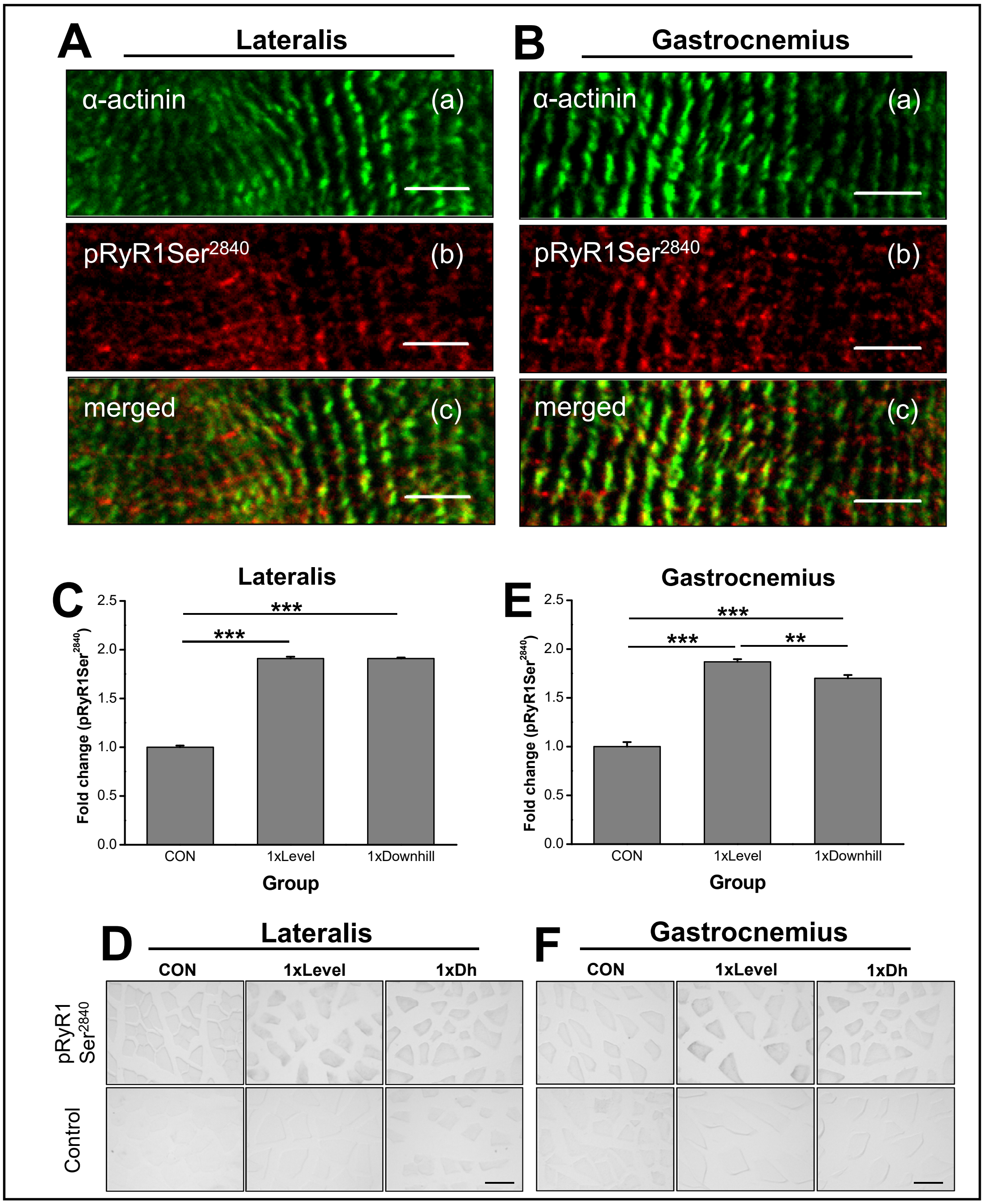

Fig. 2. Immunohistochemical analysis of pRyR1Ser^{2840} in rat LAT and GAS muscles. (A and D) Double staining against (a) α-actinin and (b) pRyR1Ser^{2840} shows localizations of Z-disks (α-actinin) in close vicinity of junctional sarcoplasmic reticuli (pRyR1Ser^{2840}) that surround t-tubuli, which are located in the transitional zone of A- and I-bands in skeletal muscles. The merged picture is demonstrated in (c). Fold changes of pRyR1Ser^{2840} in LAT (B) and GAS (E) muscle under 1xLevel and 1xDownhill conditions compared to CON conditions. pRyR1Ser^{2840} shows significantly elevated levels in both muscles after acute exercise stimulations. Representative pRyR1Ser^{2840} staining in LAT (C) and GAS (F) muscle under CON, 1xConc, and 1xEcc conditions. The upper panels depict the pRyR1Ser^{2840} pattern; the lower panel shows control slides that were incubated with 0.8% BSA instead of primary antibody. ** $p<0.01$, *** $p<0.001$. Bar in (A and D) is 5 µm, bar in (C and F) is 50 µm. In total, n=2000 muscle fibers were measured per intervention group.

Acute exercise results in increased pRyR1Ser^{2840} levels

Confocal laser scanning microscopy of longitudinal LAT and GAS skeletal muscle fibers showed localizations of Z-disks in close vicinity to junctional SRs that surround t-tubuli, which located to the transitional zone of A- and I-bands in skeletal muscles containing RyR1 (Fig. 2A, B).

LAT muscle. To test whether one single running exercise stimulus induces RyR1 phosphorylation, pRyR1Ser^{2840} was quantified in LAT muscle subjected to15 minutes of exercise by semi-quantitative immunohistochemistry. Compared to CON condition, both exercise protocols (1xLevel and 1xDownhill) resulted in significantly increased phosphorylation at Ser^{2840} of RyR1 with no difference between the two exercised groups (Fig. 2C, Supplementary Table S2). Representative immunohistochemical staining of LAT fibers are shown in Fig. 2D.

GAS muscle. Compared to the CON condition, both exercise conditions resulted in significantly increased phosphorylations of RyR1 at Ser^{2840} (Fig. 2E, Supplementary Table S2). In contrast to LAT muscle, the 1xLevel rat GAS displayed significantly higher pRyR1Ser^{2840} values compared to the 1xDownhill condition (Fig. 2E, Supplementary Table S2). Representative immunohistochemical staining of GAS fibers are shown in Fig. 2F. We further used western blot to proof our histological pRyRSer^{2840} results.

LAT muscle. The results confirm significant increases of pRyR1Ser^{2840} in both 1xLevel and 1xDownhill conditions compared to CON (Fig. 3A). Whereas these results are in general agreement with the observations obtained by immunohistochemical staining, western blot quantifications revealed significantly higher pRyR1Ser^{2840} values in 1xLevel compared to 1xDownhill condition (Fig. 3A). Representative western blot bands for pRyR1Ser^{2840} are depicted in Fig. 3I (upper panel). For quantification of relative pRyR1Ser^{2840} amounts, we measured total RyR1 levels (Fig. 3I). Since total RyR1 western blot analyses did not show any differences between the tested conditions, we normalized pRyR1Ser^{2840} to total RyR1.

GAS muscle. Western blot analysis of 1xLevel exercise showed significantly increased values of pRyR1Ser^{2840} compared to CON (Fig. 3B). Differences for 1xDownhill condition were barely below significance (Fig. 3B). These results support our observations from immunohistochemical staining (Fig. 2E). Representative western blots for pRyR1Ser^{2840} normalized to total RyR1are depicted in Fig. 3I.

RyR1-phosphorylating kinases change their activation state upon acute exercise

We further studied mechanisms that contribute to the observed pRyR1Ser^{2840} patterns upon acute exercise. We analyzed signaling molecules that are involved in RyR1 phosphorylation including pCaMKIIThr^{286}, pAktSer^{473}, and pPTENSer^{380}.

Phosphorylated calcium/calmodulin-dependent protein kinase IIThr^{286}. pCaMKIIThr^{286} is involved in the phosphorylation of RyR in heart muscle [33]. In LAT muscle we observed a pCaMKIIThr^{286} signal opposing the pRyR1Ser^{2840} pattern. Both 1xLevel and 1xDownhill exercises led to significantly increased pCaMKIIThr^{286} signals in LAT muscles (Fig. 3C, I) compared to CON, whereas 1xDownhill caused even higher pCaMKIIThr^{286} levels (Fig. 3C, I) than 1xLevel. In GAS muscle, the pCaMKIIThr^{286} signal significantly increased in both exercise groups (Fig. 3D, I) compared to CON. In contrast to LAT muscle, pCaMKIIThr^{286} signal showed highest levels upon 1xLevel (Fig. 3D, I).

Phosphorylated protein kinase B/AktSer^{473}. pAktSer^{473} directly interacts with CaMKII [34, 35], thus we measured pAktSer^{473} as a marker to confirm the pCaMKIIThr^{286} signals. In LAT muscle, pAkt^{473} levels corroborated with pCaMKIIThr^{286} results. Both 1xLevel and 1xDownhill conditions led to significantly increased phosphorylations at Ser^{473} (Fig. 3E, I) compared to CON with highest phosphorylation in the 1xDownhill group, which was significantly higher (Fig. 3E, I) compared to 1xLevel group. In GAS muscle, pAktSer^{473} levels increased upon 1xLevel (Fig. 3F, I), but decreased upon 1xDownhill compared to CON and 1xLevel (Fig. 3F, I). Consequently, pAktSer^{473} was highest upon 1xLevel stimulation (Fig. 3F, I), confirming pCaMKIIThr^{286} signals.

Cell Physiol Biochem 2019;52:633-652
DOI: 10.33594/000000045
Published online: 26 March 2019

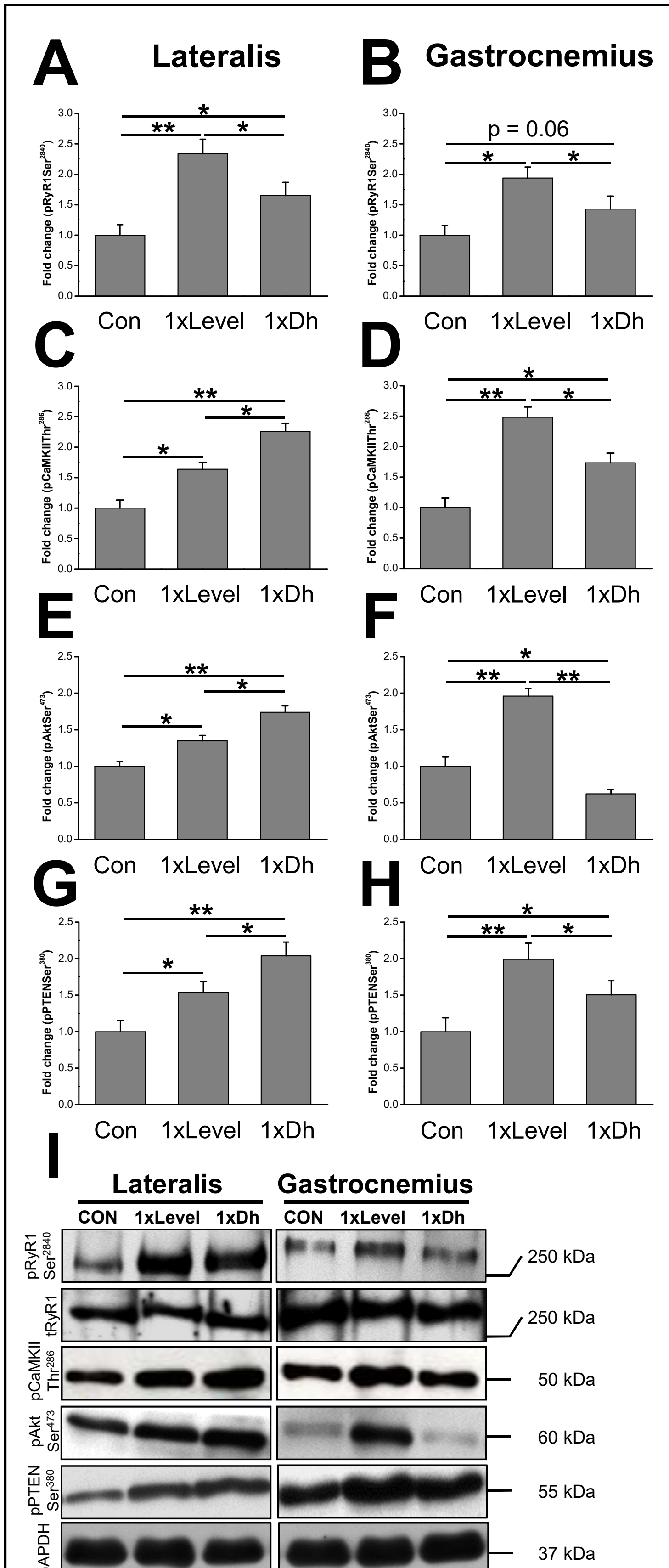

Fig. 3. Western blot analysis of RyR1 and signaling molecules in rat LAT and GAS muscles. Fold changes of pRyR1Ser2840 in LAT (A) and GAS (B) muscle upon 1xLevel and 1xDownhill compared to CON conditions show significantly elevated levels after acute exercise stimulations. Fold changes of pCaMKIIThr286 levels in LAT (C) and GAS (D) compared to CON show increased levels after acute exercise stimulations. Fold changes of pAktSer473 levels in LAT (E) and GAS (F) compared to CON. Fold changes of pPTENSer380 levels in LAT (G) and GAS (H) compared to CON show increased levels after acute exercise stimulations. Representative western blots of pRyR1Ser2840, total RyR1, pCaMKIIThr286, pAktSer473, PI3K, and pPTENSer380 as well as the internal loading control GAPDH are depicted in (I). * $p<0.05$, ** $p<0.01$. n(western blot experiments) = 8 for each tested condition.

Cell Physiol Biochem 2019;52:633-652
DOI: 10.33594/000000045
Published online: 26 March 2019

Phosphorylated phosphatase and tensin homolog deleted from chromosome 10Ser^{380}. To find a mechanistic explanation for the differences in pCaMKIIThr^{286} and pAktSer^{473} distributions between LAT and GAS muscles, we next focused on PTEN, which inhibits the kinase function of PI3K [36]. Consequently, phosphorylations of kinases downstream of PI3K, including CaMKII and Akt, are inhibited by activated PTEN. Phosphorylation at Ser^{380} directs PTEN away from the plasma membrane towards the cytosol, hence, resulting in a translocation-dependent inactivation of PTEN that permits phosphorylations of downstream kinases [36]. We found pPTENSer^{380} signals to correlate with observed pCaMKIIThr^{286} and pAktSer^{473} signals in both LAT and GAS muscles and under both exercise conditions (Fig. 3G, H, I). In agreement with pCaMKIIThr^{286} and pAktSer^{473} signals, the pPTENSer^{380} levels differed between LAT and GAS muscle (Fig. 3G, H, I), indicating that PTEN phosphorylation at Ser^{280} is most likely responsible for the Akt/CaMKII-mediated RyR1 phosphorylation.

RyR1 stabilizers dissociate from the RyR1 complex upon acute exercise

We measured PKAc associated to RyR1 and acute exercise-induced dissociations of the stabilizers calstabin-1, PDE4D3, and PP1 from RyR1 in SR membrane-enriched microsome pellets and supernatants. The stabilizers prevent RyR1 complexes from 'leaky' conditions making calstabin-1, PP1, and PDE4D3 critical players for RyR1-mediated Ca^{2+} homeostasis in skeletal muscle [8].

Catalytic subunit of protein kinase A. Besides CaMKII, protein kinase A (PKA) is a major kinase involved in RyR1 phosphorylation [9] and is activated by physical exercise [37, 38]. We quantified its catalytic subunit PKAc [9] in whole muscle homogenates. As demonstrated in Fig. 4A, we observed a significant increase of PKAc in both LAT and GAS muscle upon either exercise mode compared to CON, indicating that PKA is activated upon exercise and thus likely contributes to RyR1 phosphorylation. A direct interaction between PKAc and RyR1 is necessary to transfer the respective phosphate group. Thus, we went on to quantify PKAc in pellets (P) and supernatants (S) [9] to test whether acute exercise induced enhanced associations between RyR1 and PKAc. We did not observe any differences between PKAc(P) and PKAc(S) in both muscles (Fig. 4B, F) at CON conditions, indicative of equal PKAc distributions. However, we measured slight increases of PKAc(P) that were just below significance (Fig. 4B, F), but reached statistical significance in GAS muscle upon 1xDownhill condition (Fig. 4B, F). Together, our results indicate that acute exercise increased PKAc associated with RyR1 in SR membrane-enriched microsomes to trigger RyR1 phosphorylation.

RyR1 stabilizers. To prove our hypothesis that acute exercise results in dissociations of stabilizing molecules from RyR1, we analyzed protein levels of calstabin-1, PDE4D3, and PP1 in SR-enriched microsome pellets (P) as well as in supernatants (S). In non-exercised controls, all three stabilizers showed significantly higher abundances in P compared to S (Fig. 4C, D, E, F), indicating their associations to RyR1 complexes. In contrast, both exercise interventions caused enhanced dissociation of these stabilizers from RyR1 complexes in SR membrane-enriched microsomes of both muscles, as indicated by a significant increase in calstabin-1, PDE4D3, and PP1 levels in S compared to P (Fig. 4C, D, E, F). These data demonstrate that one single running exercise stimulus elicits effective dissociation of the stabilizers calstabin-1, PDE4D3, and PP1 from RyR1. To verify our approach of SR membrane-enriched microsome isolations containing RyR1, we demonstrate a positive RyR1 signal in the pellet fraction, while the supernatant fraction is negative for the RyR1 signal (Fig. 4G).

Acute exercise causes increased nuclear NFATc1 and epigenetic histone H3 marks

Because we observed significant RyR1 phosphorylation upon acute exercise, we tested the hypothesis that these acute exercise-induced alterations exert functional consequences.

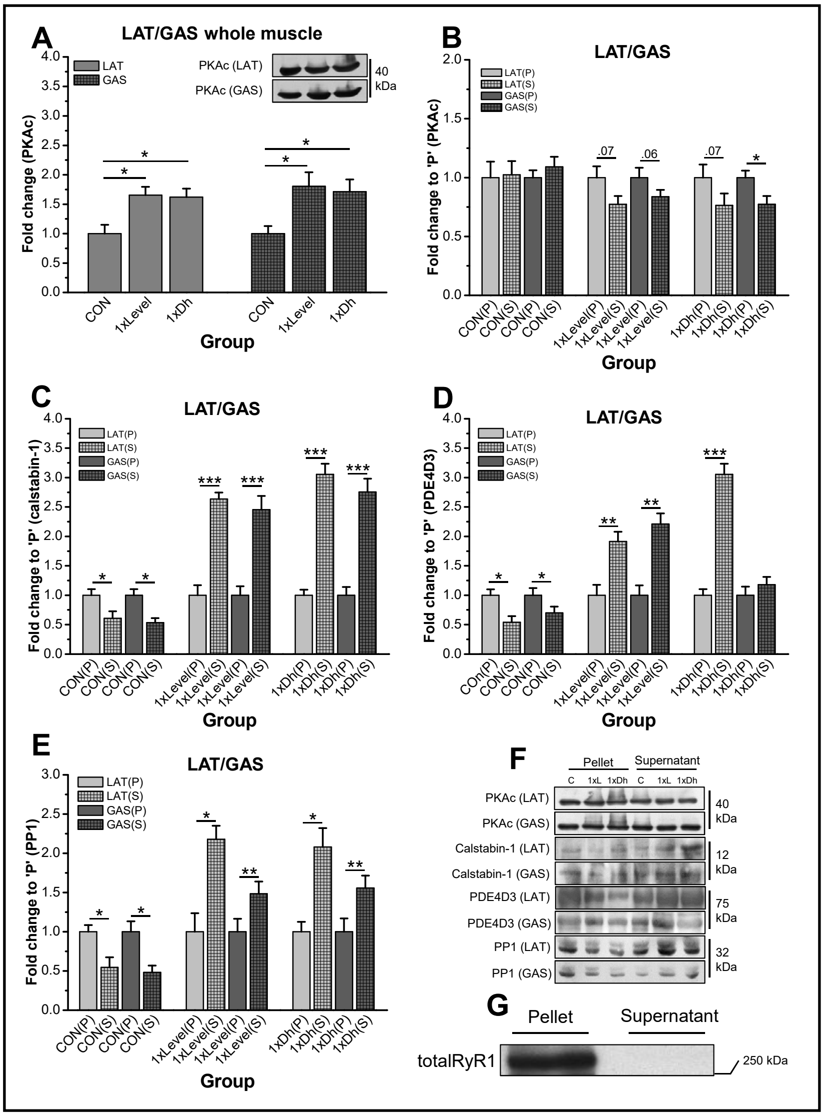

Fig. 4. PKAc, calstabin-1, PDE4D3, and PP1 regulations in LAT and GAS muscles after exercise. (A) Regulation of PKAc levels by exercise stimuli in LAT and GAS muscles. PKAc levels increased significantly after exercise programs in both muscles. Representative western blot bands are shown for PKAc (40 kDa) in both muscles. GAPDH (36 kDa) served as internal loading control (not shown). Fold changes of PKAc (B), calstabin-1 (C), PDE4D3 (D), and PP1 (E) levels in pellet and supernatant of LAT and GAS muscles relative to CON. In (B) no changes between CON pellet and supernatant were observed; however, both exercise modes resulted in a strong tendency toward increased PKAc levels in LAT pellets compared to supernatants (p=0.07 for each condition) while 1xDownhill running resulted in significantly increased PKAc levels in GAS pellets compared to supernatants. In (C), CON calstabin-1 levels were significantly higher in the pellet than in the supernatant; however, after 1xLevel and 1xDownhill stimulations, calstabin-1 levels were significantly higher in the supernatant than in the pellet. In (D), CON PDE4D3 levels were significantly higher in the pellet than in the supernatant; however, after 1xLevel and 1xDownhill stimulations, PDE4D3 levels were significantly higher in supernatant than in pellet. In (E), CON PP1 levels were significantly higher in the pellet than in the supernatant; however, after 1xLevel and 1xDownhill running, PP1 levels were significantly higher in the supernatant than in the pellet. (F) Representative western blots are shown for PKAc (40 kDa), calstabin-1 (12 kDa), PDE4D3 (75 kDa), and PP1 (33 kDa) for CON, 1xLevel and 1xDownhill conditions in pellets and supernatants of LAT and GAS muscles. (G) Western blot of total RyR1 in CON condition in pellet and supernatant of LAT muscle demonstrates that the approach of SR-enriched microsome preparation was successful. * $p<0.05$, ** $p<0.01$, *** $p<0.001$, P = pellet, S = supernatant. n(western blot experiments) = 4 for each tested condition.

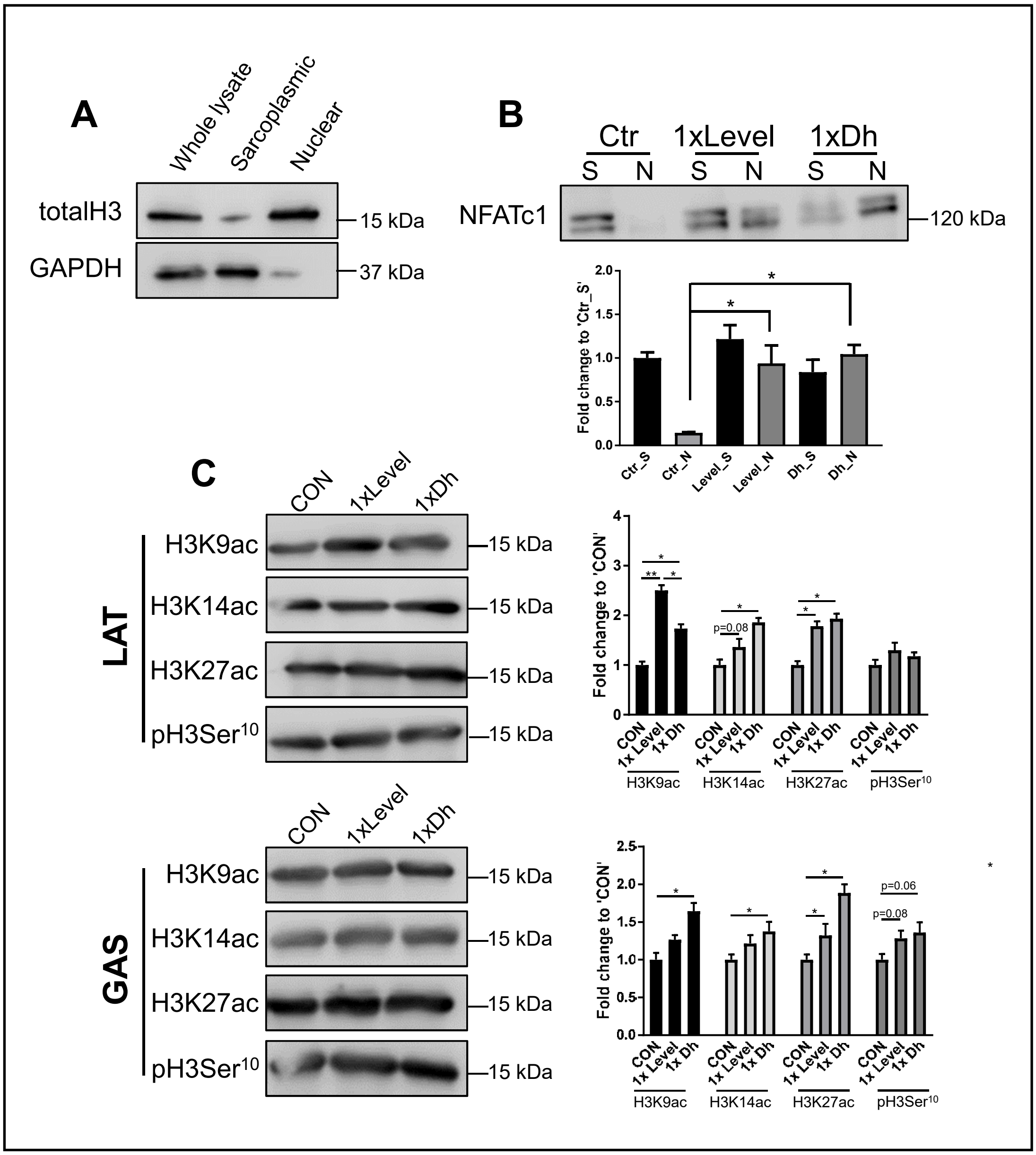

Fig. 5. Nuclear shuttling of NFATc1 and epigenetic histone H3 modifications upon acute exercise. (A) Confirmation of nuclear and sarcoplasmic fractions in skeletal muscles. We performed western blot for a nuclear marker protein (total H3) and a sarcoplasmic marker protein (GAPDH), and whole lysate, sarcoplasmic fraction, and nuclear fractions were loaded. Total H3 predominantly shows a signal in nuclear fractions, whereas GAPDH was predominantly detected in sarcoplasmic fractions. (B) NFATc1 was detected in sarcoplasmic and nuclear fractions of CON, 1xLevel, and 1xDh LAT and GAS muscles. As shown, NFATc1 abundances increased in nuclear fractions of 1xLevel and 1xDownhill compared to CON, whereas the sarcoplasmic fractions remained unchanged. The western blot shows results from LAT muscles, but is representative for GAS muscles (not shown). (C) The epigenetic histone H3 marks H3K9ac, H3K14ac, H3K27ac, and pH3Ser[10] were analyzed in nuclear fractions of LAT (upper panel) and GAS (lower panel) muscles. As shown, H3 acetylations increase with both 1xLevel and 1xDownhill, whereas pH3Ser[10] remains unchanged. n(western blot experiments) = 8 for each tested condition.

To this end, we studied the abundance of NFATc1 and histone H3 modifications between sarcoplasmic and nuclear fractions. NFATc1 is Ca^{2+}-sensitive and increased $[Ca^{2+}]_{cyt}$ rapidly triggers NFATc1 translocations into nuclei [39]. This translocation can have functional consequences, because NFATc1 acts as a *Myh7* gene-activating transcription factor [40] determining oxidative muscle fiber phenotypes.

As shown in Fig. 5A, we detected total H3 predominantly in the nuclear fraction, whereas we detected GAPDH predominantly in the sarcoplasmic fractions. We studied NFATc1 abundances in nuclear and sarcoplasmic fractions and found that sarcoplasmic NFATc1 levels remained unchanged upon acute exercises, whereas NFATc1 levels significantly increased in nuclear fractions upon both acute exercise interventions (Fig. 5B).

We further studied whether acute exercise modifies epigenetic histone H3 marks, which depend on changes in $[Ca^{2+}]_{cyt}$ [18, 19]. We focused on transcription- and elongation-initiating H3 acetylations at lysine 9 (H3K9ac), lysine 14 (H3K14ac), lysine 27 (H3K27ac) and phosphorylation at Ser^{10} ($pH3Ser^{10}$). In the nuclear fractions of LAT muscles, we observed that H3K9ac, H3K14ac, and H3K27ac were significantly increased upon both exercise programs, whereas $pH3Ser^{10}$ was not changed (Fig. 5C). In nuclear fractions of GAS muscle, we found that predominantly acute eccentric muscle contractions resulted in significantly increased H3K9ac, H3K14ac, and H3K27ac levels. $pH3Ser^{10}$ was also unchanged in GAS muscles (Fig. 5C).

Discussion

We hypothesized in this work that acute muscle contractions alter RyR1 complex assembly resulting in rapid changes of muscle phenotype-controlling machineries. We indeed found that acute muscle contractions trigger RyR1 phosphorylations that are accompanied by RyR1 stabilizer dissociations and involved signaling cascade activations. These events alter $[Ca^{2+}]_{cyt}$, which is the driving force for the observed increased NFATc1 nuclear shuttling and epigenetic H3 modifications.

Ca^{2+} oscillations play critical roles in skeletal muscle signaling, performance or weakness, because of the potential to control signaling pathways and nuclear transcription factors [41]. Detailed knowledge about early acute muscle contraction-induced modifications of RyR1 is important to understand whether acute exercise changes the local muscle Ca^{2+} homeostasis [42, 43]. This is of interest, because repetitive, but short-term acute exercise is favored to treat muscle disease-related pathologies [12], to induce metabolic improvements in muscle [44] and is advantageous over chronic exercise regimes due to longer regeneration periods [45]. Mechanistically, the analysis of molecular processes is preferable upon acute stimulations rather than long-term exercise regimes as unwanted secondary side effects can be minimized.

We demonstrate herein that acute exercise leads to increased $pRyR1Ser^{2840}$ levels in rat LAT and GAS muscles upon both predominantly concentric (level) and predominantly eccentric (downhill) contractions. Interestingly, acute level and downhill exercises caused distinct $pRyR1Ser^{2840}$ levels. This could relate to the former finding of activity-induced increases in [ATP] to activate RyR1 in both Ca^{2+}-dependent and –independent manners [46, 47]. But to gain more detailed insights into the observed $pRyR1Ser^{2840}$ patterns following acute exercise, we studied different molecular pathways that regulate RyR1, including RyR1 stabilizers and RyR1-phosphorylating signaling cascades [7, 48]. We first focused on $pCaMKIIThr^{286}$, because this kinase mediates RyR phosphorylation [33, 49] and acute exercise increases $pCaMKIIThr^{286}$ levels as fast as a few seconds lasting up to several minutes upon stimulation [50]; however, associations with RyR1 phosphorylation are unexplored. Our data support the findings of early CaMKII phosphorylation and suggest a role of CaMKII as an upstream regulator of RyR1 in muscles. Whereas RyR1 phosphorylation was highest upon 1xLevel in both LAT and GAS muscles, we found highest $pCaMKIIThr^{286}$ levels upon 1xDownhill in LAT, and upon 1xLevel stimulation in GAS. These results show the contribution of additional pathways to synergistically phosphorylate RyR1 with a dependence on contraction mode and muscle. This argument is supported by the pAktSer^{473} pattern that shows exercise mode- and muscle-dependent differences that mimic pCaMKIIThr^{286} levels indicating a direct CaMKII and Akt interaction axis [34, 35].

Due to the muscle- and exercise type-specific CaMKIIThr^{286} regulation, we further tested if the pCaMKIIThr^{286}-regulating PTEN system was also modulated in a muscle-specific and exercise type-dependent manner. We indeed found muscle- and exercise-dependent differences of pPTENSer^{380} levels. Phosphorylation of PTEN at Ser^{380} leads to its inactivation by guiding PTEN to the sarcoplasm, where it is unable to interfere with the PI3K signaling [36]. The observed pPTENSer^{380} levels confirm muscle- and exercise type-specific pCaMKIIThr^{286} and pAktSer^{473} patterns indicating the involvement of interacting upstream mechanisms, including kinases and their inhibitor regulations, to phosphorylate RyR1 upon acute exercise.

The holoenzyme PKA is activated by cAMP, which rapidly increases with exercise [37, 38] and PKA further controls RyR1 phosphorylation [9]. We observed increases of the activated catalytic PKA (PKAc) subunit and direct PKAc associations with RyR1 upon both acute exercise regimes. Thus, we show that PKA is rapidly activated by acute exercise and we identified an additional component contributing to RyR1 phosphorylation. This highlights that RyR1 is controlled by numerous means. Because the phosphorylation of RyR1 is a dynamic process, PKA might not be tethered to RyR1 permanently, which would explain its increased, but transient association to RyR1.

Unlike PKA, the RyR1 stabilizers calstabin-1, PDE4D3, and PP1 [7] form stable aggregates with RyR1, whereas their chronic dissociations from RyR1 result in uncoordinated Ca^{2+} oscillations and consequently impaired skeletal muscle functions [8]. We found significant dissociations of calstabin-1, PDE4D3, and PP1 from RyR1-containing microsomes demonstrating physiological impacts of acute exercise on molecular Ca^{2+}-regulating components. The consequence of rapid $[Ca^{2+}]_{cyt}$ changes upon acute exercise are unclear, but could trigger muscle-determining factors.

One such muscle-determining and Ca^{2+}-sensitive player is NFATc1 that has a critical function as transcription factor in oxidative muscle fiber phenotyping [17, 40, 51]. We found that NFATc1 rapidly increased its nuclear abundance upon acute exercise. This confirms earlier reports, which found that acute Ca^{2+} sparks rapidly dephosphorylate NFAT isoforms to expose their nuclear localization sequences (NLS) to stimulate nuclear NFAT imports within minutes [52, 53]. This general finding was substantiated in primary muscle cells, which were electrically stimulated and showed increased NFATc1 abundances in myonuclei within minutes [39], meaning that NFATc1 remarkable senses dynamic changes in $[Ca^{2+}]_{cyt}$ and frequencies of Ca^{2+} oscillations. This finding of rapid pRyR1Ser^{2840}-induced NFATc1 translocations is important, because it presents a physiological explanation through which mechanisms repetitive short-term exercise potentially direct skeletal muscle phenotyping. Further, NFATc1 controls cell size and intra-muscular nuclei retaining [54]. This, in combination with the MyHC gene control, demonstrates that NFATc1 is responsible for the activation of mechanisms that acutely navigate muscle repair mechanisms upon acute muscle damaging exercise, such as eccentric contractions. The mechanistic background for this physiological result is a newly established Ca^{2+} equilibrium forcing nuclear NFATc1 abundances.

A second muscle-determining and Ca^{2+}-sensitive mechanism mediates epigenetic H3 modifications. Specifically, acute (exercise-induced) changes of $[Ca^{2+}]_{cyt}$ trigger acetylations of H3 at lysine 9 (H3K9ac), lysine 14 (H3K14ac) and lysine 27 (H3K27ac) [18, 19] as well as phosphorylations of H3 (pH3Ser^{10}) [20]. These epigenetic H3 modifications can be mediated by Ca^{2+}-sensitive kinases, including CaMKII, and are associated with transcription initiation and elongation [19]. We found increased H3K9ac, H3K14ac, and H3K27ac levels upon both acute level and downhill running in both muscles. It was demonstrated in cardiac muscles that changes in Ca^{2+} oscillations result in similar H3 acetylations, which caused alternative splicing of cardiac muscle-regulating genes [19]. Another study in humans found that acute exercise increases defined H3 acetylation sites, which was accompanied by increased pCaMKIIThr^{286} levels [18]. Acute exercise did not change pH3Ser^{10} in LAT and tended to increase this modification in GAS; however, we did not identify significant values, which was surprising, because H3 acetylations relate to pH3Ser^{10}, as H3 acetylations are effectively preceded by H3 phosphorylations at Ser^{10} in *in vitro* systems [20, 55]. Our data indicate that exercise-induced H3 acetylations do not depend on H3 phosphorylations in skeletal muscles under physiological *in vivo* exercise conditions. Overall, our findings suggest that muscles subjected to acute exercise activate epigenetic machineries to rapidly stimulate transcriptional initiation and elongation to adapt to the new demands and environmental stress. The transcriptional initiation and elongation might also be linked to muscle repair mechanisms upon acute muscle-damaging exercise. It was demonstrated that epigenetic H3 modifications, including the herein investigated, contribute the maintenance of functional muscle phenotypes upon damage [56, 57]. The basic concept about how acute exercise determines RyR1 phosphorylation, its regulating kinases, its stabilizers and functional Ca^{2+}-dependent effector is schematically presented in Fig. 6 (Fig. 6A: sedentary conditions; Fig. 6B: acute exercise condition).

We further observed that eccentric exercise caused lower pRyR1Ser^{2840} levels compared to concentric exercise. This was particularly unexpected, because muscles experience higher mechanical strain (see Fig. 1) and a higher number of fibers is innervated as reflected by increased VO_2 values during eccentric compared to concentric muscle work (see Supplementary Fig. S1) [58, 59]. Our data cannot explain this phenomenon in detail, but we suggest that lower maximum force peaks combined with increased passive forces induced by intra-sarcomeric protein interactions [60] to attenuate activation of Ca^{2+}-regulating components, including RyR1, during eccentric work. Exposing skeletal muscles to higher eccentric stresses (with the same peak force as in concentric exercise) could test this assumption. Furthermore, we measured a sarcomere length of about 3.2 µm upon eccentric exercise. This enhanced sarcomere length still allows for active contractions, which are supported by passive forces as demonstrated in isolated muscle fibers [60, 61] wherefore it might reflect physiological sarcomere length upon acute eccentric muscle contractions *in vivo*. *In vitro* single muscle fiber studies revealed that increased muscle force correlates with acutely increased RyR1 phosphorylation [16], which is in contrast to chronic training [8]. Transferred to our results, it is plausible that acute *in vivo* muscle loading acutely increased muscle forces due to transient, but not chronic RyR1phosphorylations. This assumption is supported by data from our group showing increased passive muscle forces in cardiomyocytes upon acute exercise [62]. This has a practical relevance in the way that molecular cascades finally trigger physiological outcomes, here transiently increased muscle force. Recently, it was demonstrated that strenuous acute exercise potentially causes RyR1 fragmentations that consequently disturb the Ca^{2+} homeostasis and related muscle contraction mechanisms [63]. However, we did not observe any comparable RyR1 fragmentations reflecting physiologically tolerable loading by the applied exercise programs and hence rather physiological than disturbed Ca^{2+} oscillations. A pathological condition of altered Ca^{2+} is inflammation. We can connect our results to inflammation in the way acute inflammation as expressed by increases of the pro-inflammatory cytokine IL-1 negatively controls $[Ca^{2+}]_{cyt}$ by blocking RyR1 and hence retaining Ca^{2+} inside the SR. IL-1 exerts its inhibitory effects on RyR1 by direct interactions with RyR1 rather than through indirect mechanisms [64]. Chronic inflammatory processes, e.g. rheumatoid arthritis, are accompanied by high reactive oxygen/nitrogen species (ROS/RNS). ROS/RNS were identified as modifiers of RyR1 into a 'leaky' state, comparable to the phosphorylated state [3, 10]. Thus, chronic inflammation induces continuously high $[Ca^{2+}]_{cyt}$ that result in muscle dysfunction. Collectively, skeletal muscle dysfunctions under acute and chronic conditions might be linked to non-physiological control of the RyR1. Our data provide *in vivo* evidence for early and rapid phosphorylation of skeletal muscle RyR1 in physiological acute exercise model induced different signaling pathways and accompanied by RyR1 stabilizer dissociations. Of note, we observed increased nuclear abundances of $[Ca^{2+}]_{cyt}$-sensitive NFATc1 and increased $[Ca^{2+}]_{cyt}$-sensitive epigenetic H3 modifications,

Cell Physiol Biochem 2019;52:633-652
DOI: 10.33594/000000045
Published online: 26 March 2019

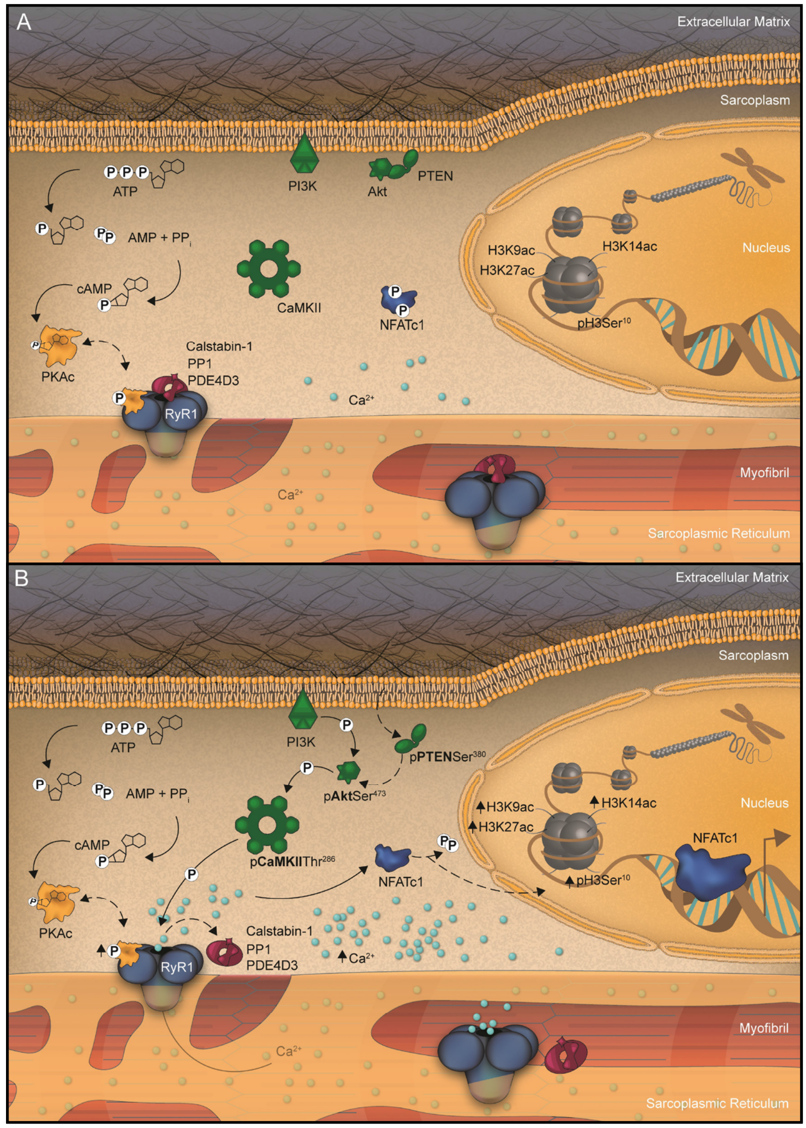

Fig. 6. Summary of RyR1 phosphorylation-triggered signaling and mediated NFATc1 and epigenetic histone H3 modifications induced by acute exercise. (A) Under resting conditions, the ATP metabolism is low as is the cAMP concentration. Therefore, only small amounts of the apoenzyme PKA are cleaved into its active catalytic isoform, PKAc. Subsequently, RyR1 phosphorylation is low, but not absent, and the RyR1 stabilizing molecules, calstabin-1, PDE4D3, and PP1, are associated to RyR1. In parallel, resting conditions result in low inactive (phosphorylated) forms of PTEN. Likewise, there is little activation of Akt at Ser^{473} and, thus, of CaMKII at Thr^{286}. This results in the regular oscillation of Ca^{2+} from RyR1, similar to what occurs in the event of low PKAc. The consequences are sarcoplasmic NFATc1 localizations as well as low epigenetic H3 acetylations/phosphorylations. (B) Acute in vivo exercise induces high ATP metabolism in working skeletal muscles resulting in increased cAMP levels. This event activates the apoenzyme PKA to be cleaved into its catalytic isoform, PKAc. Subsequently, RyR1 phosphorylation increases and its stabilizing molecules, calstabin-1, PDE4D3, and PP1, show transient dissociations from RyR1. In parallel, acute exercise leads to increased levels of the inactive (phosphorylated) form of PTEN, enabling Akt to be PI3K-phosphorylated at Ser^{473} (bold). Subsequently, CaMKII is activated at Thr^{286}, which might amplify the PKAc-mediated RyR1 phosphorylation. Consequently, NFATc1 is dephosphorylated and translocates into the nucleus and H3 is epigenetically modified by specific acetylations. Synergistically, these events control skeletal muscle properties and molecular phenotypes even under conditions of acute and short-term muscle work.

which are associated with increased transcriptional initiation and elongation. These findings demonstrate that acute exercise rapidly evokes critical physiological consequences making acute exercise bouts a crucial determinant that orchestrates of muscle function and properties.

Conclusion

Proper Ca^{2+} oscillations are essential for physiological skeletal muscle properties [7]. Detailed knowledge about mechanisms controlling Ca^{2+} oscillations and consequences of altered Ca^{2+} oscillations is hence critical to understand muscle function. Our data show that acute exercise phosphorylates the Ca^{2+} oscillation-controlling RyR1 channel. We further identify different signaling pathways that concertedly phosphorylate RyR1 and thus likely control Ca^{2+} oscillations. The action of involved signals is amplified by dissociations of calstabin-1, PDE4D3, and PP1 from RyR1 complexes causing rapidly modified RyR1. The physiological consequences of these acute exercise-induced RyR1 modifications are (i) enhanced nuclear abundances of the muscle phenotype-controlling transcription factor NFATc1 and (ii) epigenetic modifications of the histone H3 associated with transcriptional initiation and elongation. Consequently, we demonstrate for the first time that physiological and acute exercise bouts evoke alterations of the local muscle milieu to determine novel functional equilibria expressed by nuclear NFATc1 and H3 modifications.

Acknowledgements

FS designed the study and performed experiments, collected, analyzed and interpreted data, financial support, wrote the manuscript. KB performed experiments, approved the manuscript. MV performed experiments, approved the manuscript. WB performed experiments, analyzed data, approved the manuscript. The authors thank Bianca Collins and Mojgan Ghilav (Department of Molecular and Cellular Sport Medicine) for technical assistance as well as Dr. Raphael Rastetter (Institute of Biochemistry I, Medical School, University of Cologne) for provision of the ultracentrifuge. The authors thank Anncharlott Berglar, PhD (Scientific & Medical Illustration Service, abc-images.com) for her expertise in image creation (Fig. 6). This study was supported by grants of the Partnership for Clean Competition (to FS) and the Federal Ministry of Education and Research (BMBF, to FS).

Disclosure Statement

The authors declare that they have no competing interests.

References

1 Cheng H, Lederer WJ: Calcium sparks. Physiol Rev 2008;88:1491–1545.

2 Melov S, Tarnopolsky MA, Beckman K, Felkey K, Hubbard A: Resistance exercise reverses aging in human skeletal muscle. PLoSOne 2007;2:e465.

3 Andersson DC, Betzenhauser MJ, Reiken S, Meli AC, Umanskaya A, Xie W, Shiomi T, Zalk R, Lacampagne A, Marks AR: Ryanodine receptor oxidation causes intracellular calcium leak and muscle weakness in aging. Cell Metab 2011;14:196–207.

4 Goonasekera SA, Lam CK, Millay DP, Sargent MA, Hajjar RJ, Kranias EG, Molkentin JD: Mitigation of muscular dystrophy in mice by SERCA overexpression in skeletal muscle. J Clin Invest 2011;121:1044–1052.

5 Andersson DC, Meli AC, Reiken S, Betzenhauser MJ, Umanskaya A, Shiomi T, D'Armiento J, Marks AR: Leaky ryanodine receptors in beta-sarcoglycan deficient mice: a potential common defect in muscular dystrophy. Skelet Muscle 2012;2:9.
6 van Deutekom JC, van Ommen GJ: Advances in Duchenne muscular dystrophy gene therapy. Nat Rev Genet 2003;4:774–783.
7 Bellinger AM, Mongillo M, Marks AR: Stressed out: the skeletal muscle ryanodine receptor as a target of stress. J Clin Invest 2008;118:445–453.
8 Bellinger AM, Reiken S, Dura M, Murphy PW, Deng SX, Landry DW, Niemand D, Lehnart SE, Samaru M, LaCampagne A, Marks AR: Remodeling of ryanodine receptor complex causes "leaky" channels: a molecular mechanism for decreased exercise capacity. Proc Natl Acad Sci U S A 2008;105:2198–2202.
9 Reiken S, LaCampagne A, Zhou H, Kherani A, Lehnart SE, Ward C, Huang F, Gaburjakova M, Gaburjakova J, Rosemblit N, Warren MS, He KL, Yi GH, Wang J, Burkhoff D, Vassort G, Marks AR: PKA phosphorylation activates the calcium release channel (ryanodine receptor) in skeletal muscle: defective regulation in heart failure. J Cell Biol 2003;160:919–928.
10 Bellinger AM, Reiken S, Carlson C, Mongillo M, Liu X, Rothman L, Matecki S, Lacampagne A, Marks AR: Hypernitrosylated ryanodine receptor calcium release channels are leaky in dystrophic muscle. NatMed 2009;15:325–330.
11 Gehlert S, Bungartz G, Willkomm L, Korkmaz Y, Pfannkuche K, Schiffer T, Block W, Suhr F: Intense resistance exercise induces early and transient increases in ryanodine receptor 1 phosphorylation in human skeletal muscle. PLoS One 2012;7:e49326.
12 Tjønna AE1, Lee SJ, Rognmo Ø, Stølen TO, Bye A, Haram PM, Loennechen JP, Al-Share QY, Skogvoll E, Slørdahl SA, Kemi OJ, Najjar SM, Wisløff U: Aerobic interval training versus continuous moderate exercise as a treatment for the metabolic syndrome: a pilot study. Circulation 2008;118:346–354.
13 Sveen ML, Jeppesen TD, Hauerslev S, Kober L, Krag TO, Vissing J: Endurance training improves fitness and strength in patients with Becker muscular dystrophy. Brain 2008;131:2824–2831.
14 Little JP, Safdar A, Wilkin GP, Tarnopolsky MA, Gibala MJ: A practical model of low-volume high-intensity interval training induces mitochondrial biogenesis in human skeletal muscle: potential mechanisms. J Physiol 2010;588:1011–1022.
15 Calabria E, Ciciliot S, Moretti I, Garcia M, Picard A, Dyar KA, Pallafacchina G, Tothova J, Schiaffino S, Murgia M: NFAT isoforms control activity-dependent muscle fiber type specification. Proc Natl Acad Sci U S A 2009;106:13335–13340.
16 Andersson DC, Betzenhauser MJ, Reiken S, Umanskaya A, Shiomi T, Marks AR: Stress-induced increase in skeletal muscle force requires protein kinase A phosphorylation of the ryanodine receptor. J Physiol 2012;590:6381–6387.
17 Hogan PG, Chen L, Nardone J, Rao A: Transcriptional regulation by calcium, calcineurin, and NFAT. Genes Dev 2003;17:2205–2232.
18 McGee SL, Fairlie E, Garnham AP, Hargreaves M: Exercise-induced histone modifications in human skeletal muscle. J Physiol 2009;587:5951–5958.
19 Sharma A, Nguyen H, Geng C, Hinman MN, Luo G, Lou H: Calcium-mediated histone modifications regulate alternative splicing in cardiomyocytes. Proc Natl Acad Sci 2014;111:E4920–E4928.
20 Whitlock JP, Augustine R, Schulman H: Calcium-dependent phosphorylation of histone H3 in butyrate-treated HeLa cells. Nature 1980;287:74–76.
21 Hamann N, Kohler T, Muller R, Bruggemann GP, Niehoff A: The Effect of Level and Downhill Running on Cortical and Trabecular Bone in Growing Rats. Calcif Tissue Int 2012; DOI:10.1007/s00223-012-9593-6.
22 Hamann N, Zaucke F, Heilig J, Oberländer KD, Brüggemann GP, Niehoff A: Effect of different running modes on the morphological, biochemical, and mechanical properties of articular cartilage. Scand J Med Sci Sports 2014;24:179–188.
23 Butterfield TA, Leonard TR, Herzog W: Differential serial sarcomere number adaptations in knee extensor muscles of rats is contraction type dependent. J Appl Physiol 2005;99:1352–1358.
24 Ogilvie RW, Armstrong RB, Baird KE, Bottoms CL: Lesions in the rat soleus muscle following eccentrically biased exercise. Am J Anat 1988;182:335–346.
25 Whitehead NP, Weerakkody NS, Gregory JE, Morgan DL, Proske U: Changes in passive tension of muscle in humans and animals after eccentric exercise. J Physiol 2001;533:593–604.

26 Westerlind KC, Byrnes WC, Mazzeo RS: A comparison of the oxygen drift in downhill vs. level running. J Appl Physiol 1992;72:796–800.
27 Wang HV, Chang LW, Brixius K, Wickstrom SA, Montanez E, Thievessen I, Schwander M, Müller U, Bloch W, Mayer U, Fässler R: Integrin-linked kinase stabilizes myotendinous junctions and protects muscle from stress-induced damage. JCell Biol 2008;180:1037–1049.
28 Greiwe L, Vinck M, Suhr F: The muscle contraction mode determines lymphangiogenesis differentially in rat skeletal and cardiac muscles by modifying local lymphatic extracellular matrix microenvironments. Acta Physiol (Oxf) 2015;217:61–79.
29 Suhr F: Detection of fusion events in Mammalian skeletal muscle. Methods Mol Biol 2015;1313:115–129.
30 Giannini G, Conti A, Mammarella S, Scrobogna M, Sorrentino V: The ryanodine receptor/calcium channel genes are widely and differentially expressed in murine brain and peripheral tissues. J Cell Biol 1995;128:893–904.
31 Zhang X, Tallini YN, Chen Z, Gan L, Wei B, Doran R, Miao L, Xin HB, Kotlikoff MI, Ji G: Dissociation of FKBP12.6 from ryanodine receptor type 2 is regulated by cyclic ADP-ribose but not beta-adrenergic stimulation in mouse cardiomyocytes. Cardiovasc Res 2009;84:253–262.
32 Lee SH, Kim BJ, Park DR, Kim UH: Exercise induces muscle fiber type switching via transient receptor potential melastatin 2-dependent Ca^{2+} signaling. J Appl Physiol 2018;124:364–373.
33 Zalk R, Lehnart SE, Marks AR: Modulation of the ryanodine receptor and intracellular calcium. Annu Rev Biochem 2007;76:367–385.
34 Wei Y, Williams JM, Dipace C, Sung U, Javitch JA, Galli A, Saunders C: Dopamine transporter activity mediates amphetamine-induced inhibition of Akt through a Ca2+/calmodulin-dependent kinase II-dependent mechanism. Mol Pharmacol 2007;71:835–842.
35 Fujikawa K, Kawakami A, Tanaka F, Iwamoto N, Tamai M, Eguchi K: Calcium/calmodulin-dependent protein kinase II (CaMKII) regulates tumour necrosis factor-related apoptosis inducing ligand (TRAIL)-mediated apoptosis of fibroblast-like synovial cells (FLS) by phosphorylation of Akt. Clin Exp Rheumatol 2009;27:952–957.
36 Das S, Dixon JE, Cho W: Membrane-binding and activation mechanism of PTEN. Proc Natl Acad Sci U S A 2003;100:7491–7496.
37 Chasiotis D: The regulation of glycogen phosphorylase and glycogen breakdown in human skeletal muscle. Acta Physiol Scand Suppl 1983;518:1–68.
38 Graham TE, Helge JW, MacLean DA, Kiens B, Richter EA: Caffeine ingestion does not alter carbohydrate or fat metabolism in human skeletal muscle during exercise. J Physiol 2000;529:837–847.
39 Kubis HP, Scheibe RJ, Meissner JD, Hornung G, Gros G: Fast-to-slow transformation and nuclear import/export kinetics of the transcription factor NFATc1 during electrostimulation of rabbit muscle cells in culture. J Physiol 2002;541:835–847.
40 Serrano AL, Murgia M, Pallafacchina G, Calabria E, Coniglio P, Lomo T, Schiaffino S: Calcineurin controls nerve activity-dependent specification of slow skeletal muscle fibers but not muscle growth. Proc Natl Acad Sci U S A 2001;98:13108–13113.
41 Berchtold MW, Brinkmeier H, Muntener M: Calcium ion in skeletal muscle: its crucial role for muscle function, plasticity, and disease. Physiol Rev 2000;80:1215–1265.
42 Culligan K, Banville N, Dowling P, Ohlendieck K: Drastic reduction of calsequestrin-like proteins and impaired calcium binding in dystrophic mdx muscle. J Appl Physiol 2002;92:435–445.
43 Dulhunty AF, Beard NA, Pouliquin P, Kimura T: Novel regulators of RyR Ca2+ release channels: insight into molecular changes in genetically-linked myopathies. J Muscle Res Cell Motil 2006;27:351–365.
44 Burgomaster KA, Howarth KR, Phillips SM, Rakobowchuk M, MacDonald MJ, McGee SL, Gibala MJ: Similar metabolic adaptations during exercise after low volume sprint interval and traditional endurance training in humans. J Physiol 2008;586:151–160.
45 Gibala MJ, Little JP, Macdonald MJ, Hawley JA: Physiological adaptations to low-volume, high-intensity interval training in health and disease. J Physiol 2012;590:1077–1084.
46 Meissner G: Adenine nucleotide stimulation of Ca2+-induced Ca2+ release in sarcoplasmic reticulum. J Biol Chem 1984;259:2365–2374.
47 Meissner G, Darling E, Eveleth J: Kinetics of rapid Ca2+ release by sarcoplasmic reticulum. Effects of Ca2+, Mg2+, and adenine nucleotides. Biochemistry 1986;25:236–244.

Cell Physiol Biochem 2019;52:633-652
DOI: 10.33594/000000045
Published online: 26 March 2019

48 Lanner JT, Georgiou DK, Joshi AD, Hamilton SL: Ryanodine receptors: structure, expression, molecular details, and function in calcium release. Cold Spring Harb Perspect Biol 2010;2:a003996.
49 Witcher DR, Kovacs RJ, Schulman H, Cefali DC, Jones LR: Unique phosphorylation site on the cardiac ryanodine receptor regulates calcium channel activity. J Biol Chem 1991;266:11144–11152.
50 Rose AJ, Kiens B, Richter EA: Ca2+-calmodulin-dependent protein kinase expression and signalling in skeletal muscle during exercise. J Physiol 2006;574:889–903.
51 Kubis HP, Scheibe RJ, Meissner JD, Hornung G, Gros G: Fast-to-slow transformation and nuclear import/export kinetics of the transcription factor NFATc1 during electrostimulation of rabbit muscle cells in culture. J Physiol 2002;541:835–847.
52 Loh C, Carew JA, Kim J, Hogan PG, Rao A: T-cell receptor stimulation elicits an early phase of activation and a later phase of deactivation of the transcription factor NFAT1. Mol Cell Biol 1996;16:3945–3954.
53 Timmerman LA, Clipstone NA, Ho SN, Northrop JP, Crabtree GR: Rapid shuttling of NF-AT in discrimination of Ca2+ signals and immunosuppression. Nature 1996;383:837–840.
54 Perroud J, Bernheim L, Frieden M, Koenig S: Distinct roles of NFATc1 and NFATc4 in human primary myoblast differentiation and in the maintenance of reserve cells. J Cell Sci 2017;130:3083–3093.
55 Lo WS, Duggan L, Emre NC, Belotserkovskya R, Lane WS, Shiekhattar R, Berger SL: Snf1--a histone kinase that works in concert with the histone acetyltransferase Gcn5 to regulate transcription. Science 2001;293:1142–1146.
56 Moresi V, Marroncelli N, Coletti D, Adamo S: Regulation of skeletal muscle development and homeostasis by gene imprinting, histone acetylation and microRNA. Biochim Biophys Acta 2015;1849:309–316.
57 Liu L, Cheung TH, Charville GW, Hurgo BMC, Leavitt T, Shih J, Brunet A, Rando TA: Chromatin Modifications as Determinants of Muscle Stem Cell Quiescence and Chronological Aging. Cell Rep 2013;4:189–204.
58 Armstrong RB, Ogilvie RW, Schwane JA: Eccentric exercise-induced injury to rat skeletal muscle. J Appl Physiol 1983;54:80–93.
59 Schwane JA, Armstrong RB: Effect of training on skeletal muscle injury from downhill running in rats. J Appl Physiol 1983;55:969–975.
60 Leonard TR, Herzog W: Regulation of muscle force in the absence of actin-myosin-based cross-bridge interaction. Am J Physiol Cell Physiol 2010;299:C14–C20.
61 Herzog W: The role of titin in eccentric muscle contraction. J Exp Biol 2014;217:2825–2833.
62 Muller AE, Kreiner M, Kotter S, Lassak P, Bloch W, Suhr F, Krüger M: Acute exercise modifies titin phosphorylation and increases cardiac myofilament stiffness. Front Physiol 2014;5:449.
63 Place N, Ivarsson N, Venckunas T, Neyroud D, Brazaitis M, Cheng AJ, Kamandulis S, Girard S, Volungevičius G, Paužas H, Mekideche A, Kayser B, Martinez-Redondo V, Ruas JL, Bruton J, Truffert A, Lanner JT, Skurvydas A, Westerblad H: Ryanodine receptor fragmentation and sarcoplasmic reticulum Ca2+ leak after one session of high-intensity interval exercise. Proc Natl Acad Sci U S A 2015;112:15492–15497.
64 Friedrich O, Yi B, Edwards JN, Reischl B, Wirth-Hücking A, Buttgereit A, Lang R, Weber C, Polyak F, Liu I, von Wegner F, Cully TR, Lee A, Most P, Völkers M: IL-1α Reversibly Inhibits Skeletal Muscle Ryanodine Receptor. A Novel Mechanism for Critical Illness Myopathy? Am J Respir Cell Mol Biol 2014;50:1096–1106.